Sources of Gas-Discharge Plasma: Effect of the Absorbed Dose and Active Particle Composition on Physicochemical Transformations in Biological Substrates

DOI: 10.17691/stm2018.10.2.10
Received May 29, 2017

© **I.M. Piskarev,** PhD, Leading Reseracher[1];
K.A. Astaf'eva, Junior Researcher, Department of Physicochemical Researches, Central Scientific Research Laboratory[2];
I.P. Ivanova, DSc, Head of the Department of Physicochemical Researches, Central Scientific Research Laboratory[2]

[1]Skobeltsyn Institute of Nuclear Physics, Lomonosov Moscow State University, 1 Leninskiye Gory, Moscow, 119991, Russia;
[2]Privolzhsky Research Medical University, 10/1 Minin and Pozharsky Square, Nizhny Novgorod, 603005, Russia

The aim of the investigation was to study the effect of the absorbed dose and composition of active particles of various gas-discharge plasma sources on physicochemical changes in biological substrates.

Materials and Methods. A generator of flash corona electrical discharge plasma, pulsed sources of plasma radiation Pilimin IR-10, Pilimin IR-1, and Brig, OUFK-01 Solnyshko quartz ultraviolet irradiator with a DKB-9 low-pressure mercury lamp served as the sources of gas-discharge plasma. The radiation dose was measured using a Fricke dosimeter. Optical density of the solutions was registered with the help of SF-102 spectrophotometer. Fluorat-02 Panorama spectrophotometer was used to study fluorescence spectra of tryptophan in the aqueous solution at 10 mg/L concentration after treatment with gas-discharge plasma sources. Concentration of sulfhydryl (–SH) groups before and after irradiation with Pilimin IR-10 and DKB-9 UV lamp was determined for aqueous solutions of albumin and methemoglobin.

Results. Emission spectra of the generator of flash corona electrical discharge plasma and spark discharge plasma in the air for Pilimin IR-10 generator have been analyzed. The spectral data show that plasma of the spark electrical discharge is weakly ionized, thermal radiation serves as the main acting factor.

A wide peak in the range of ~360 nm region, where there is a peak of nitrous acid NO_2^- absorption, is observed in the spectra of water samples exposed to plasma radiation of Pilimin IR-10, Pilimin IR-1, and Brig generators. The peak has a structure connected with the formation of nitrogen compounds of a more complicated nature. Increase of radiation pulse duration results in the increase of optical density at the wavelengths less than 330 nm. 355–360 nm peak height relative to the substrate does not practically change.

Under the action of the mercury lamp radiation, hydrogen peroxide and NH_4^+ ions are generated in water.

The highest absorption dose is noted after the treatment with flash corona electrical discharge plasma, the lowest with radiation of the DKB-9 UV lamp and Brig generator.

The concentration of –SH-groups in tryptophan, albumin, and methemoglobin increases when exposed to plasma radiation. The absorbed dose generated by the Pilimin IR-10 generator exceeds 4.5 times the dose generated by the UV lamp, i.e. the effect is caused by a specific reaction mechanism and is not connected directly with the dose.

Conclusion. The main role in the alterations in biological substrates exposed to various plasma sources is played by the composition of the active particles generated by the source. These data allow the development of more effective gas-discharge devices for biomedical purposes and can be employed for implementation of innovation plasma technologies in medicine.

Key words: gas-discharge plasma; gas-discharge devices; plasma radiation sources; plasma technologies in medicine.

Introduction

In the last decade, medical and biological effects of cold gas-discharge plasma and plasma radiations have actively been studied and devices based on gas-discharge technologies have been created [1–3]. These are plasma generators and generators of various types of plasma, which are the sources of active particles.

Barrier discharge, creeping arc discharge, spark discharge, and corona electric discharge are used in plasma generators. Sources of plasma radiation are electrical discharge lamps, quartz mercury lamp, in

Corresponding author: Igor M. Piskarev, e-mail: i.m.piskarev@gmail.com

particular, UV light-emitting diodes, generators of spark discharge in air [4, 5].

Primary plasma active particles are generated immediately in plasma, which is in contact with the treated object, and directly react with organic matters of the object biological substrates. Plasma radiation affects the object distantly (contact-free, non-invasively), while primary active particles are generated under the influence of radiation in the substrate and react further with its matters. Plasma radiation represents photons, which passing through the air (λ>200 nm) and hitting the object are, firstly, absorbed and activate type I and II reactions with the initiator in a triplet state, and, secondly, participate in the formation of active forms of oxygen and nitrogen [6–8].

Products formed under the action of plasma or plasma radiation can be detected by spectrophotometric and chemical methods in aqueous solutions of organic and inorganic matters. If there are no initiators in the aqueous solution and if there is no possibility of direct absorption of photons by the molecules of the dissolved matters, active forms of oxygen and nitrogen are generated under the influence of radiation directly in the water. It is these active particles that initiate chemical transformations of the organic substrates [8].

Biomedical devices based on gas-discharge technologies [4, 9] differ in such parameters as discharge power, pulse duration, photon flux, composition of generated active particles, and so on. The biological effects (e.g. cytotoxic effect, and others) induced by different plasma sources are expressed to a more or less degree. But at the same time, the role of the dose (the energy absorbed by the specimen) and specific reactions initiated by the generated particles remain unexplored. The analysis of the absorbed dose effect on the biological substrates exposed to various radiation sources will permit optimization of radiation characteristics, a more directional influence on a chemical or biological process, and the development of effective innovation technologies on the basis of gas-discharge plasma in medicine.

To assess the role and composition of active particles in concrete reactions, it is necessary to analyze the composition of the generated particles, mechanisms of reactions initiated by the particles of different types, radiation doses (the energy released in the specimen), and also to compare biochemical effects after the exposure to the gas-discharge lamp and plasma radiation.

The aim of the study was to study the effect of the absorbed dose and the composition of active particles of various sources of gas-discharge plasma on physicochemical transformations in biological substrates.

Materials and Methods

Sources of active particles

Generator of flash corona electrical discharge plasma. The generator (Figure 1) represents a glass vessel 90 mm in diameter and 0.5 L volume, which is closed with a fluoroplastic cover. 7 discharge electrodes from stainless steel 2 mm in diameter are inserted through the cover along the edges of the vessel. A ground electrode of the same material is inserted in the center of the cover. The discharge electrodes are located at a distance of 6.1–6.2 mm from the surface of the treated liquid. The ground electrode runs to the very bottom of the vessel. The electrode is placed in a fluoroplastic tube and contacts the liquid only at the vessel bottom. The liquid volume is 49 ml, its amount is determined by the necessity to provide the required distance between the discharge electrodes and the liquid surface. The liquid layer is 10 mm thick.

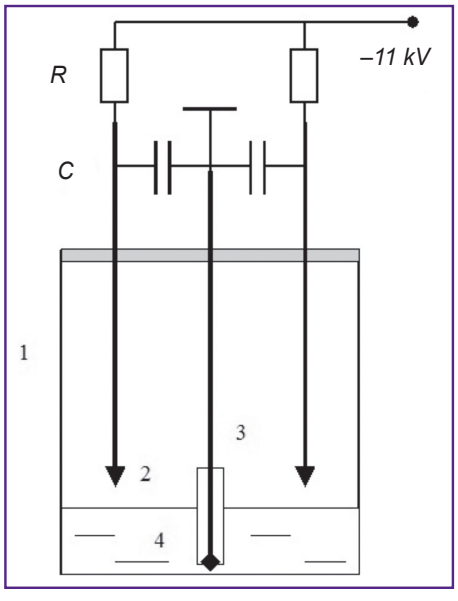

Figure 1. Schematic diagram of the generator of flash corona electrical discharge plasma:
(*1*) reaction vessel; (*2*) discharge electrodes; (*3*) ground electrode; (*4*) treated liquid

Each discharge electrode is grounded via *C*=30 pF capacitor. A high voltage (11 kV) of negative polarity is supplied to them via the resistor (*R*=20 MΩ). Under these conditions, a flash corona electrical discharge is generated on the electrode [10]. Pulse repetition frequency is ~100 kHz, current pulse amplitude up to 2 mA, average discharge current to each electrode 70 μA. The electrons emitted by the corona discharge produce the so-called electron wind, i.e. a flow of electrons from the electrode point to the water surface. The electrons impact the gas molecules and impart the pulse to them. As a result, a directional movement of ionized gas towards the liquid occurs. The electron wind transfers the active particles generated in the discharge region to the liquid surface. Pits appear in the liquid opposite each electrode. The pulsed character of the discharge and the electron wind provide mixing

of the liquid layer almost to the full depth [10]. It is very important for the ground electrode to contact with the liquid only at the bottom otherwise mixing will be very weak.

Thus, when a generator of flash corona electrical discharge plasma is used, active particles are generated in the region of the discharge and transferred by the electron wind to the liquid surface. On the surface, the active particles interact with the substrate, the interaction products are mixed with the entire liquid.

Pilimin IR-10, Pilimin IR-1 generators of pulsed plasma radiation. In these generators (Skobeltsyn Institute of Nuclear Physics, Lomonosov Moscow State University), the energy is accumulated in the capacitor and is released in the air gap [11, 12] (Figure 2). The capacitor *C* is charged from 11 kV high voltage source via a ballast resistor *R*. A breakdown voltage of the air gap, to which the capacitor is connected, is equal to 6 kV. When voltage in the capacitor exceeds 6 kV, a breakdown occurs, a spark discharge appears. When the capacitor is completely run down, the discharge ceases and the capacitor starts to be charged again. In Pilimin IR-10, *C*=3.3 nF, *R*=MΩ, discharge pulse duration is 150 μs, pulse repetition frequency — 10 Hz. The energy released in the discharge during one pulse amounts to 0.059 J, in a second to 0.59 J. In Pilimin IR-1, the value of *C*=0.1 μF, *R*=3 MΩ, pulse duration is 1500 μs, pulse repetition frequency 1 Hz. The energy released in a discharge during 1 pulse amounts to 1.8 J. Duration of the pulse leading edge of both generators is ~50 ns.

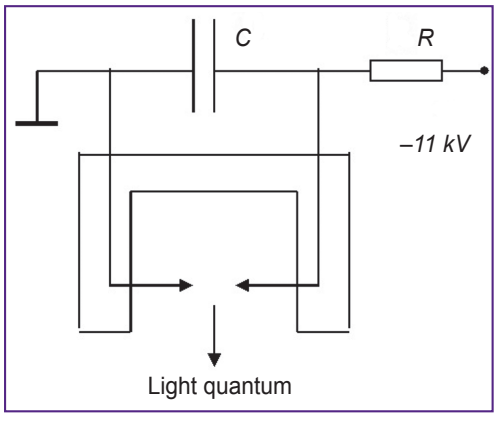

Figure 2. Schematic diagram of the discharge circuit of the plasma radiation generators Pilimin IR-1 and Pilimin IR-10

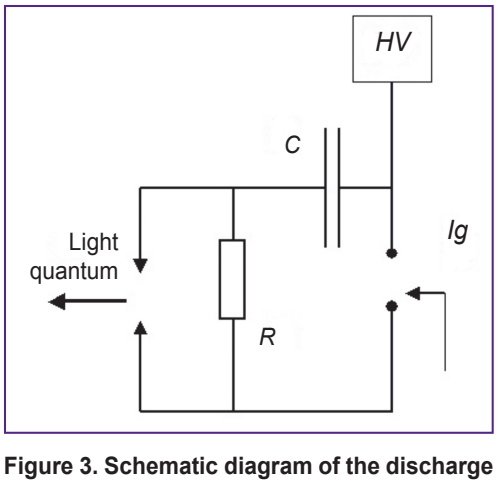

Figure 3. Schematic diagram of the discharge circuit of the Brig plasma radiation generator

Brig pulsed plasma radiation source [13]. In the Brig generator (Russian Federal Nuclear Center — All-Russian Research Institute of Experimental Physics, Sarov, Nizhny Novgorod region) (Figure 3), a high voltage is supplied to the capacitor *C*=0.1 μs from a charging unit *HV*. Once the desired voltage of 10 kV is achieved, the charging unit is switched off. A triggered vacuum gap *Ig* is closed with the preset 1 Hz frequency. The capacitor discharges through the resistor *R*=75 Ω. When the gap is closed, a voltage pulse is formed with a 10 kV amplitude, 50 ns leading edge, and duration up to 4 μs, which is applied to the spark gap. Pulse repetition frequency is 1 Hz. The energy released in the spark gap is equal to 5 J.

OUFK-01 Solnyshko quartz ultraviolet irradiator. A 9W DKB-9 low-pressure mercury lamp is used in the irradiator (Solnyshko, Russia). The lamp operates in a continuous mode, emits a monochromatic radiation with a wavelength of 253.7 nm. The photon flux is equal, according to the specification, to I_0=5.4·10^{-8} mol(cm^2·s)$^{-1}$ at a distance of 3 cm from the lamp surface.

Fricke dosimeter. It represents an aqueous solution of Mohr's salt (2 g/L) ([Fe^{2+}]=5.1·10^{-3} mol/L) in 0.4 M sulfuric acid and 50 mg/L NaCl. The dosimeter is traditionally used to study ionizing radiation. In the reactions with active particles generated under the action of ionizing radiation, bivalent iron is oxidized to a trivalent form. The concentration of the trivalent iron being formed is measured by the optical band density λ=304 nm, ε=2100 L(mol·cm)$^{-1}$ [14]. If the average energy necessary for generation of an oxidizing particle is known, the energy absorbed by the solution may be determined by the optical density of the λ=304 nm band, i.e. the concentration of the trivalent iron formed is proportional to the energy released in the solution. The optical density of the solutions was registered using SF-102 spectrophotometer (Aquilon, Russia), the quartz cuvette was 10 mm thick.

Fluorescence measurement. Fluorescence spectra of tryptophan were measured using Fluorat-02 Panorama spectrophotometer (Lumex, Russia). For tryptophan, the excitation wavelength of 288 nm and registration wavelength of 350 nm have been determined experimentally. Fluorophores are known to quench their own fluorescence [15] therefore the tryptophan concentration has also been determined experimentally. Dependence of fluorescence on tryptophan concentration was measured for this purpose. At low

concentrations, the fluorescence increases linearly, reaches saturation, and begins to diminish. For our work, there was chosen the concentration corresponding to the middle part of the initial linear dependence region, which amounted to ~0.05 mmol/L.

Determination of –SH-groups concentration. Ellman's reagent 5,5-dithiobis-(2-nitrobenzoic acid), or DTNB [15], phosphate buffer: 0.1 M Na_2HPO_4, pH 8; denaturing buffer: 7 M urea in 0.1 M Na_2HPO_4, pH 8–8.5; Ellman's reagent solution: (4 mg DTNB)/(1 ml phosphate buffer); 5% aqueous solution of albumin ($7.7 \cdot 10^{-4}$ M) as a sample were used in the work. Measurements were done in the following way.

At first, 100 µl of Ellman's solution and 100 µl of the examined sample were added to 3 ml denaturing buffer. Then it was stirred, incubated for 5 min, and photometry performed against the solution of denaturing buffer at λ=412 nm (D_{sample}). Optical density was determined spectrophotometrically using SF-102 device (the cuvette was 10 mm thick). Further, optical density was measured at the same wavelength for the control solution: 3 ml denaturing buffer, 100 ml phosphate buffer, and 100 µl Ellman's solution (D_{DTNB}). The optical density corresponding to the quantity of –SH-groups in the examined sample was $D_{SH}=D_{sample}-D_{DTNB}$. The concentration of –SH-groups after the exposure to the radiation of Pilimin IR-10 and UV lamp was determined for albumin (50 g/L) and methemoglobin (1.4 g/L) based on the extinction coefficient 13,700 $M^{-1} \cdot cm^{-1}$ [16].

Analysis of the active particle composition. The analysis was carried out by the discharge radiation spectra, specific reaction in the solution, and absorption spectra of distilled water samples exposed to the plasma and radiation sources. Radiation spectra of the generators were measured using FSD10 mini-spectrometer with a fiber input (Scientific Technical Center of Fiber-Optic Devices, Russia). To determine the concentration of hydrogen peroxide, titanium trichloride, which was prepared by the solution of 0.3 g metallic titanium in 50 ml of concentrated hydrochloric acid, was introduced into the sample. 0.1 ml of titanium trichloride solution was added to the treated water sample. The samples were treated in two Petri dishes with 18 ml total volume. Titanium trichloride was added to the treated water to identify the peroxide. The titanium compound and hydrogen peroxide form a complex having a maximum in the absorption spectrum at λ=410 nm. The hydrogen peroxide solutions of known concentration, in which $TiCl_3$ was added, were used to calibrate the spectrum. The content of NH_4^+ ions was identified using Nessler's reagent. The solutions of ammonium salts of known concentration were used to calibrate.

Water samples were exposed to plasma of flash corona electrical discharge in the reactor (see Figure 1), solution volume amounted to 49 ml; in other cases, it was performed in a Petri dish 40 mm in diameter, 5 ml solution volume. Fluorescence spectra were measured using Fluorat-02 Panorama spectrophotometer. Absorption spectra and optical density of the solutions at a certain wavelength were registered with SF-102 spectrophotometer (the quartz cuvette was 10 mm thick). Chemically pure reagents and distilled water, pH 5.5, were used in the work. The pH value was measured with Expert-001 device (Econix, Russia).

Experiment results

Active particle composition of the gas-discharge devices. To assess the composition of active particles generated by each source, spectra of plasma radiation were measured in the wavelength range of 180–1000 nm and absorption spectra of distilled water samples exposed to plasma or plasma radiation in the wavelength range of 250–400 nm.

The generator of flash corona electrical discharge plasma. It is known that the main active particles generated under the action of flash corona electrical discharge in air are $OH^{\bullet}$, $HO_2^{\bullet}$, $NO^{\bullet}$ radicals, ozone, and hydrogen peroxide [17]. On the plasma radiation spectrum of flash corona electrical discharge (Figure 4 (a)), it is seen that radiation is concentrated in the 280–380 nm wavelength interval. $OH^{\bullet}$, $HO_2^{\bullet}$, $NO^{\bullet}$ radicals are displayed in this region. Their lifetime is 10^{-7}–10^{-9} s. There is no radiation in the 200–280 nm UV-C region of the spectrum.

Short-lived radicals brought into the treated water with the electron wind decay interacting with each other. Water is the decomposition product of $OH^{\bullet}$, $HO_2^{\bullet}$ radicals, ozone, and hydrogen peroxide. The only stable product, which can be formed after $NO^{\bullet}$ radical decay, are NO_3^- ions. To detect the products formed in the water, a 49 ml water sample was exposed to a flash corona electrical discharge for 1 h. In the absorption spectrum of the exposed solution (Figure 5), the peak of absorption is observed at ~300 nm wavelength. NO_3^- ions are absorbed at this wavelength. The extinction coefficient of this peak was determined by measuring the absorption spectrum of 0.01 M $NaNO_3$ solution: ε=7 $L(mol \cdot cm)^{-1}$. The optical density A of the band with λ=300 is 0.013±0.001 units of optical density. It corresponds to the concentration of $[NO_3^-]=(1.86\pm0.15) \cdot 10^{-3}$ mol/L. The measured value of the sample pH was 2.8±0.1. The concentration of NO_3^- ions complies with the measured sample acidity.

Radiation of the DBK-9 low-pressure mercury lamp of the OUFK-01 Solnyshko irradiator. There are no sensitizers in pure distilled water and the probability of photon direct absorption at λ=253.7 nm is very small. Therefore the only mechanism of interaction of photons with water is formation of $HO_2^{\bullet}$ ions first detected in [11]. These radicals interacting with each other form hydrogen peroxide. Obtained absorption spectra of pure hydrogen peroxide solution, the absorption spectrum of the sample immediately after irradiation with the lamp for 5 h, and the same probe treated with UV radiation after the addition of titanium trichloride to it (Figure 6) allow

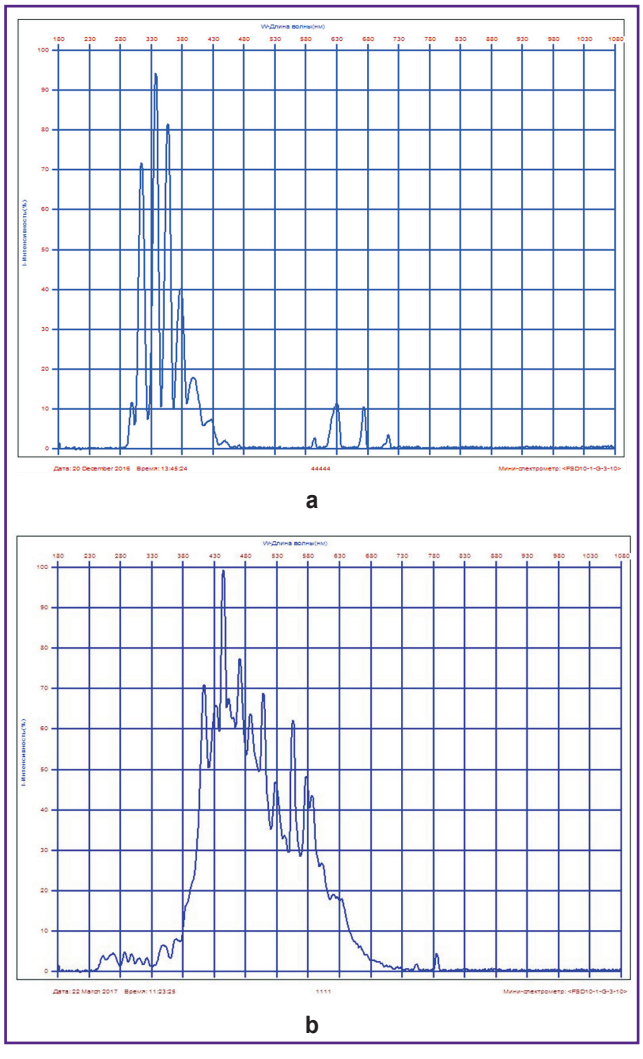

Figure 4. Radiation spectra:
(a) generator of flash corona electrical discharge plasma; (b) Pilimin IR-10 generator of spark discharge plasma radiation; when measuring the spectra, the amplification in the registration channel was adjusted so that the maximal intensity of the line was near 100%

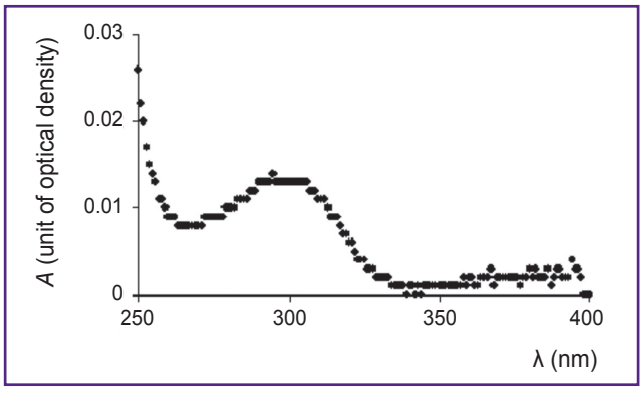

Figure 5. The absorption spectrum of distilled water treated with flash corona electrical discharge plasma for 1 h

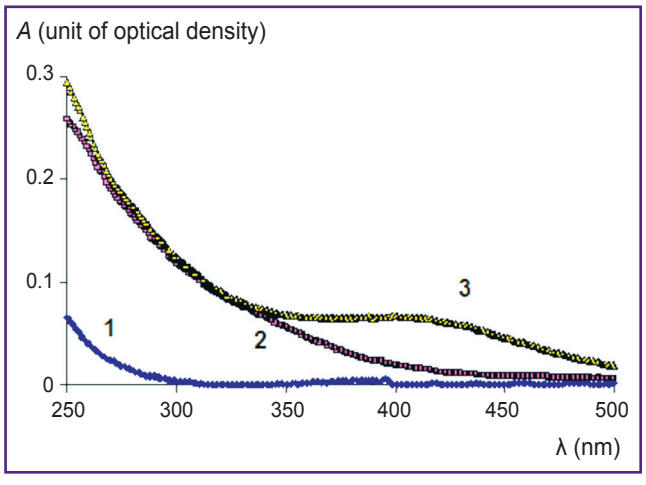

Figure 6. Identification of hydrogen peroxide in the water sample exposed to the UV mercury lamp radiation:
(*1*) 0.01% pure hydrogen peroxide; (*2*) water sample exposed to UV radiation for 5 h; (*3*) the sample exposed for 5 h and supplemented with 0.1 ml $TiCl_3$

determination of hydrogen peroxide concentration in the water sample exposed to the mercury lamp radiation for 5 h: $[H_2O_2]=(0.006\pm0.001)\%$ or $2\cdot10^{-3}$ mol/L. Hydrogen peroxide yield under the action of DKB-9 lamp radiation amounts to $(1.0\pm0.2)\cdot10^{-7}$ mol$(L\cdot s)^{-1}$.

Optical density of the water exposed to UV radiation for 5 h in 250–400 nm wavelength range (Figure 6, *curve 2*) is essentially greater of the optical density of the pure hydrogen peroxide solution (Figure 6, *curve 1*) though the concentration of the pure peroxide in this sample is higher. This means that other compounds are also formed under the action of UV radiation lamp. In the reaction with Nessler's reagent, NH_4^+ ions were found. Their concentration was about 10^{-4} g/L.

Spectra of plasma radiation and sample absorption

Plasma radiation spectra. Three sources of gas-discharge plasma radiation were used in the work: Pilimin-10, Pilimin-1, and Brig, which differ by the discharge pulse duration and energy released in the pulse. The acting factor in all sources is thermal radiation of the plasma filament heated by the electric discharge. Thermal radiation spectrum begins from the lower border of air transmission in the ultraviolet region (λ=200 nm) and covers the entire spectrum of visible radiation.

The electric discharge, during which chemically active particles can be generated, may be divided into two phases. The first one is a discharge leading edge. During this time, electric field strength in the gap between the electrodes is maximal. Potential difference between the electrodes is about 6 kV. The probability of highly excited particles (radicals) is great. The second phase is the main current pulse propagation. During this time, the spark channel represents a heated conductor. Potential difference between the electrodes

is about 100 V. The electric field in the discharge channel is minimal. The active particles generated in the first phase are spent in the interactions with each other therefore at this stage the spark channel is a source of chemically active particles (radicals), while in the second phase it is a source of UV radiation of the heated black body and stable products of chemical transformations. The stable products get on the treated object. Thus, the object (water in this experiment) undergoes the action of plasma radiation, and it is into the object (water) that the products generated in the second discharge phase get.

The radiation spectrum of the spark discharge plasma in air for Pilimin IR-10 generator is presented in Figure 4 (b). The main radiation lines are concentrated in the region of 380–550 nm wavelength. Here there are excitation lines of N_2 and O_2 molecules. There are no peaks in the region where excitation lines of ions and radicals may be located (280–380 nm). In 200–280 nm UV-C region, a wide peak of thermal radiation is observed. Thus, the spectral data show that plasma of the spark electrical discharge is weakly ionized, ions and radicals are not generated in it. The main acting factor is thermal radiation.

Discharge radiation in the visible 380–550 nm range caused by the decay of the excited N_2 and O_2 molecules is low-active. In 200–280 nm UV-C region, the discharge plasma radiates like a heated black body. It is not possible to compare the line intensity in various spectrum regions on the basis of Figure 4 (b) as in the visible region the lines are narrow, the radiation energy is concentrated in the narrow spectral regions and therefore the amplitude of the peaks is large. In UV-C region, where the radiation of the heated black body has a continuous spectrum, energy concentration in the narrow spectral range may be essentially smaller, while a total energy transmitted by the radiation is greater. Therefore the amplitude appears to be small. Under these conditions, when the line width is different, it is not correct to compare the radiation energy in various spectral ranges based on the radiation amplitude lines.

Absorption spectra of the treated water samples. To assess the composition of the products generated in the water exposed to plasma radiation, 5 ml water samples were irradiated by Pilimin IR-10, Pilimin IR-1, and Brig. For the Pilimin IR-10 generator, irradiation was performed both with an open discharge cavity and the cavity closed by quartz glass transmitting only UV radiation and not transmitting the products generated by the electric discharge. The absorption spectra were measured in 250–400 nm wavelength range immediately after the exposure and the next day (Figure 7).

In all spectra, a wide peak is observed in the region of ~360 nm — here there is an absorption peak of nitrous acid NO_2^-. This suggests that the main primary product generated under the action of each source radiation is nitrous acid. The peak structure is connected with formation of nitrogen compounds of a more complicated nature. They cannot be referred to nitrosamines, which give one wide peak with 355–360 nm maximum in this spectral region. Nitrous acid is not stable therefore 360 nm peak amplitude rapidly decreases and the peak disappears in a day. But the next day, ~300 nm peak becomes more prominent due to the contribution of nitric acid ions NO_3^-. Hence it may be concluded that exposure to the gas-discharge plasma radiation results in formation of unstable nitrous acid, which is converted to nitric acid. Attention should be paid to the fact that compounds giving the absorption peak in 360 nm region are not formed under the action of the mercury lamp radiation (λ=253.7 nm) (see Figure 6).

Compounds giving absorption in the region less than 330 nm are formed in the discharge itself and get into water by diffusion. It is signified by a great decrease of the optical density in the wavelength region less than 330 nm when the discharge cavity is closed with a quartz glass (Figure 7 (c) and (d)). The yield of compounds contributing to the optical density at λ<330 nm increases with the increase of discharge pulse duration. Pulse duration, being the longest for Pilimin IR-1 (1500 μs), is essentially shorter for Pilimin IR-10 (150 μs) and is the shortest for Brig (4 μs). It may be explained by the yield increase of the products generated in the second discharge phase with the increase of pulse duration.

Measurements of the absorbed dose. The absorbed dose was determined using a Fricke dosimeter. The concentration of trivalent iron formed in the bivalent iron solution exposed to the action of each considered sources of active particles is presented in Figure 8. The curves show the linear dependence of $[Fe^{3+}]$ on the exposure time in all cases.

It is possible to identify the quantity of oxidizers which have reacted with bivalent iron and oxidized it to the trivalent by the optical density of 304 nm band. The number of oxidizers is proportional to the energy released in the aqueous solution exposed to radiation. Therefore the yield of trivalent iron ions is proportional to the radiation energy (radiation dose) absorbed by the solution. The highest dose is noted in the sample treated with plasma of flash corona electrical discharge, the lowest dose is observed after the exposure to the DKB-9 UV lamp and Brig generator.

Chemical transformations induced by the plasma generators and sources of plasma radiation

Destruction of tryptophan. Tryptophan is established to be destroyed under the action of the gas-discharge devices used in the work. When tryptophan is disintegrated its fluorescence diminishes. The decrease of tryptophan fluorescence after the exposure to different sources of active particles has been investigated. Dependence of fluorescence on the exposure time is shown in Figure 9. It is seen that the greatest decrease of fluorescence occurs under the action of flash corona electrical discharge plasma, the weakest decrease under the radiation of the UV lamp and Brig generator.

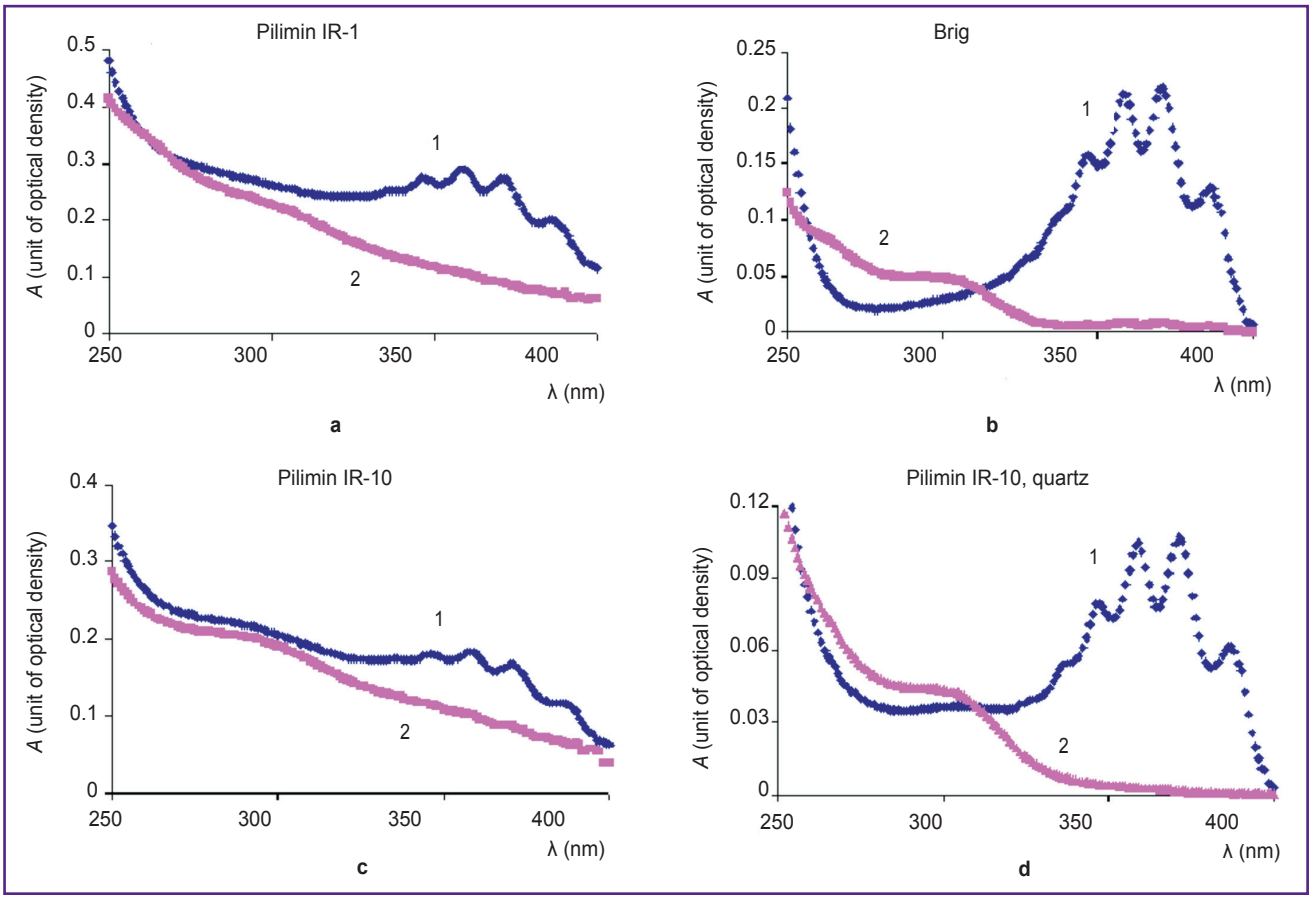

Figure 7. Absorption spectra of the water samples exposed to the spark discharge plasma radiation of various devices: (a) Pilimin IR-1; (b) Brig; (c) Pilimin IR-10, open discharge cavity; (d) Pilimin IR-10, the discharge cavity is closed with a quartz glass; (*1*) the spectrum immediately after exposure; (*2*) the spectrum the day after exposure

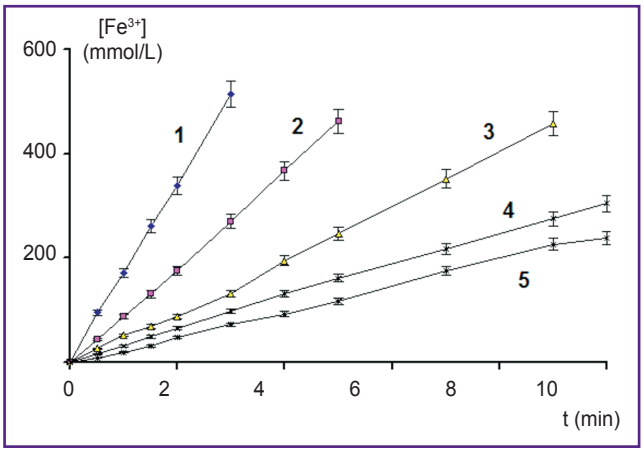

Figure 8. Concentration of trivalent iron after the exposure of Fricke solution to various sources:
(*1*) flash corona discharge plasma; (*2*) Pilimin IR-10 generator; (*3*) Pilimin IR-1; (*4*) Brig; (*5*) DKB-9 UV lamp

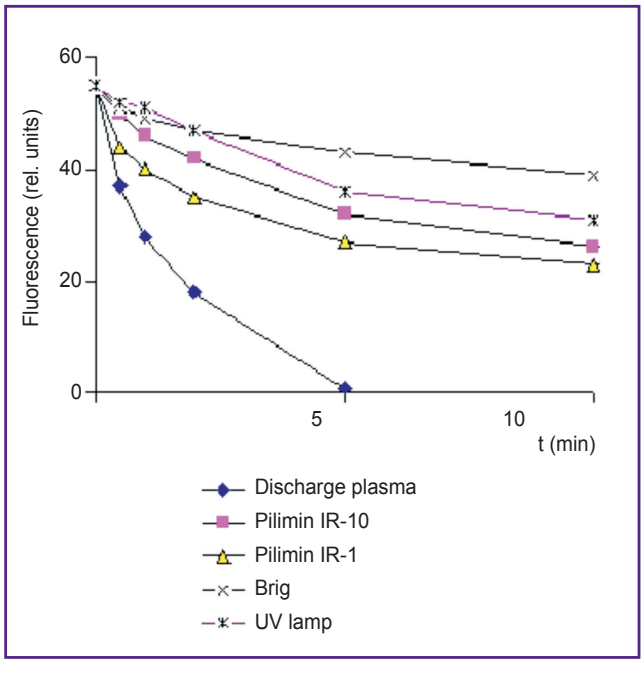

Figure 9. Dependence of tryptophan fluorescence on the time of exposure to the active particle sources

Comparison of Figures 8 and 9 showed that the extent of tryptophan destruction correlates with the value of the absorbed dose. It leads to the conclusion

that the destruction process is caused by the absorbed dose.

Reduction of –SH-groups. Let us consider the process in which the effect is determined by the properties of concrete particles. Reduction of –SH-groups in methemoglobin and albumin solutions exposed to radiation of Pilimin IR-10 and DKB-9 UV lamp has been investigated.

After methemoglobin sample has been treated by Pilimin IR-10 radiation for 30 min, the content of –SH-groups in one methemoglobin molecule grew from 7 to 9.6±0.8, while after the treatment by UV radiation for the same time it increased to 10.1±0.8.

Untreated albumin contains, on average, 0.20±0.03 –HS-groups per a molecule. After the exposure to Pilimin IR-10 radiation for 30 min, their content increases to 0.36±0.04, and after the exposure to UF radiation for the same time to 1.5±0.1. Thus the yield of the reduced –SH-groups is much higher under the action of UV radiation though the absorbed dose generated by Pilimin IR-10 exceeds 4.5 times that of the UV lamp. It means that in this case the effect is determined by the specific reaction mechanism and is not connected directly with the dose.

Discussion

The investigations performed make it possible to describe the main characteristics (the composition) of the active particles generated under the impact of various gas-discharge sources.

The characteristics of the devices used in this work and the products generated under the action of these devices in water are summarized in the Table. The results are given on the basis of the findings obtained in the course of this study and from the literature cited here.

The composition and yields of oxidizers generated in the flash corona electrical discharge have been investigated in [10, 17]. In our experiments, the yields of the particles at 100 eV energy released in the discharge are: ozone — 130 molecules, $OH^{\bullet}$ — 20 radicals, nitrogen compounds — 5 molecules.

The mechanism of active particle generation under the action of UV-C radiation was proposed in [11] and considered in detail in [8]. In case of a pulsed source of electrical discharge radiation at a high instantaneous radiation density occurring during the discharge pulse, the following mechanism of active particle generation under the action of UV-C radiation flash through the excited states of water molecules is possible [8]:

$$H_2O+h\nu \rightarrow H_2O^*; \quad (1)$$

$$H_2O^*+H_2O^* \rightarrow HO_2^{\bullet}+H_2+H^{\bullet}; \quad (2)$$

$$H^{\bullet}+O_2+M \rightarrow HO_2^{\bullet}+M \text{ (M — particle 3);} \quad (3)$$

$$H^{\bullet}+H^{\bullet}+M \rightarrow H_2+M. \quad (4)$$

Under the actions of photons, excited water molecules are formed (reaction 1), which due to their instantaneous density interact with each other (reaction 2). The energy expended in one interaction act

Description of gas-discharge devices, active particles, and products generated in water

Description	Generator type				
	Plasma	Pilimin IR-10	Pilimin IR-1	Brig	Mercury UV lamp
Discharge type	Flash corona	Spark	Spark	Spark	Arc
Discharge power (W)	7	0.59	1.8	5	9
Sample volume (ml)	49	5	5	5	5
Pulse duration (μs)	0.2	150	1500	4	Continuous radiation
Repetition frequency (Hz)	100,000	10	1	1	Continuous radiation
Average photon flux (mol(cm^2·s)$^{-1}$)	No photons	$(1.26\pm0.20)\cdot10^{-10}$	Not identified	Not identified	$5.4\cdot10^{-8}$
Photon flux in the pulse (mol(cm^2·s)$^{-1}$)	Not identified	$(1.2\pm0.2)\cdot10^{-7}$	Not identified	Not identified	Not identified
Primary particles	$OH^{\bullet}$, O_3	$HO_2^{\bullet}$, $O^{\bullet}$, N_2O	$HO_2^{\bullet}$, $O^{\bullet}$, N_2O	$HO_2^{\bullet}$, $O^{\bullet}$, N_2O	$HO_2^{\bullet}$
Secondary particles	$HO_2^{\bullet}$, NO_3^-	NO_2^-, NO_3^-	NO_2^-, NO_3^-	NO_2^-, NO_3^-	H_2O_2, NH_4^+
Fe^{2+} oxidation rate (mol(L·s)$^{-1}$)	$(2.8\pm0.3)\cdot10^{-6}$	$(1.5\pm0.2)\cdot10^{-6}$	$(8.0\pm1.0)\cdot10^{-7}$	$(5.0\pm1.0)\cdot10^{-7}$	$(4.0\pm0.5)\cdot10^{-7}$
$OH^{\bullet}$ radical yield (mol(L·s)$^{-1}$)	$(2.1\pm0.3)\cdot10^{-6}$	No	No	No	No
Ozone yield (mol(L·s)$^{-1}$)	$(1.3\pm0.2)\cdot10^{-5}$	No	No	No	No
$HO_2^{\bullet}$ radical yield (mol(L·s)$^{-1}$)	Not identified	$(1.2\pm0.3)\cdot10^{-6}$	Not identified	Not identified	$(1.1\pm0.5)\cdot10^{-6}$
NH_4^+ yield (mol/L·s)	No	$(1.7\pm0.5)\cdot10^{-10}$	Not identified	Not identified	$(2.5\pm1.5)\cdot10^{-8}$
NO_2^- + NO_3^- yield (mol(L·s)$^{-1}$)	$(5.2\pm0.4)\cdot10^{-7}$	$(5.8\pm1.6)\cdot10^{-7}$	Not identified	Not identified	No
Concentration of [...ONOOH...$ONOO^-$] complex (mol/L)	No	$(2.5\pm0.5)\cdot10^{-3}$	Not identified	Not identified	No

on active particle formation (reaction 2) is significantly greater than that expended under the action of one photon. In case of reaction 2, two fronts participate in the act of active particle formation. This condition is not satisfied for the continuous photon beam. The probability of interaction of excited H_2O^* molecules with each other for the continuous beam will be low due to a small instantaneous density of the excited water molecules, and the yield of reactions (2), (3), (4) will be smaller.

There are dissolved gases in the water: nitrogen and oxygen. The energy of UV photon with λ<250 nm is enough to accomplish the following processes:

$$N_2+O_2+\gamma \rightarrow N_2O+O^{\bullet}; \quad (5)$$

$$O_2+\gamma \rightarrow 2O^{\bullet}. \quad (6)$$

The interaction of N_2O molecules and $HO_2^{\bullet}$ radicals results further in formation of nitrous and nitric acids [8]. Processes (5) and (6) are impossible under the action of the λ=253.7 nm mercury lamp.

Thus, $HO_2^{\bullet}$ radicals, $O^{\bullet}$ atoms and N_2O molecules are supposed to be the primary active particles generated in water exposed to pulsed UV-C radiation of Pilimin IR-1, Pilimin IR-10, and Brig generators. The interaction of $HO_2^{\bullet}$ radicals may lead to formation of hydrogen peroxide however these radicals are consumed mainly in the reactions with nitrogen-containing compounds. Therefore under the action of the pulsed radiation sources, hydrogen peroxide yield appears to be low, less than the detection limit of the method used by us to identify hydrogen peroxide.

Nitrogen-containing compounds are not formed under the action of mercury lamp radiation, therefore, hydrogen peroxide was detected in the water exposed to it.

Formation of […ONOOH … $ONOO^-$] complex identified in [18] has been found to dissociate during about 2 weeks into peroxynitrite and peroxynitrous acid, which are unstable and rapidly decompose to nitric acid. The peak structure in 360 nm region may be associated with this complex. The nitrous acid and nitrosamines give a wide absorption line and cannot give the observed structure.

Conclusion

The composition of the generated active particles plays the main role in the transformations in biological substrates exposed to various gas-discharge plasma sources. Knowledge of the effect produced by different radiation sources and the role of separate particles in biochemical transformations will allow the development of more effective gas-discharge devices for biomedical purposes, and can be employed for implementation of innovation plasma technologies in medicine.

Study funding and conflicts of interest. The work was not supported by any sources, and there are no conflicts of interest related to the present study.

References

1. Fridman A. *Plasma chemistry.* Cambridge University Press; 2008, https://doi.org/10.1017/cbo9780511546075.

2. Laroussi M. Low-temperature plasmas for medicine? *IEEE Transactions on Plasma Science* 2009; 37(6): 714–725, https://doi.org/10.1109/tps.2009.2017267.

3. Baldanov B.B., Semenov A.P., Ranzhurov T.V., Nikolaev E.O., Gomboeva S.V. Action of plasma jets of a low-current spark discharge on microorganisms (Escherichia coli). *Technical Physics* 2015; 60(11): 1729–1731, https://doi.org/10.1134/s1063784215110043.

4. Astafyeva K.A., Ivanova I.P. Analysis of cytotoxic effects of medical gas-discharge devices. *Sovremennye tehnologii v medicine* 2017; 9(1): 115–122, https://doi.org/10.17691/stm2017.9.1.15.

5. Arkhipova E.V., Ivanova I.P. The effect of non-coherent impulse radiation on functional status of mononuclear cells in experiment. *Sovremennye tehnologii v medicine* 2013; 5(1): 27–31.

6. Rohatgi-Mukherjee K.K. *Fundamentals of photochemistry*. Publisher New Age International. New Delhi; 2013; 386 p.

7. Pattison D.I., Davies M.J. Actions of ultraviolet light on cellular structures. In: *Cancer: cell structures, carcinogens and genomic instability.* Birkhäuser-Verlag; 2006; p. 131–157, https://doi.org/10.1007/3-7643-7378-4_6.

8. Piskarev I.M. Active factors of low ionised plasma radiation produced in air spark discharge. *Research Journal of Pharmaceutical, Biological and Chemical Sciences* 2016; 7(4): 1171–1189.

9. Ivanova I.P., Zaslavskaya M.I. Biocydic effect of the spark discharge non-coherent impulse radiation in experiments in vitro and in vivo. *Sovremennye tehnologii v medicine* 2009; 1: 28–31.

10. Piskarev I.M. Choice of conditions of an electrical discharge for generating chemically active particles for the decomposition of impurities in water. *Technical Physics* 1999; 44(1): 53–58, https://doi.org/10.1134/1.1259251.

11. Ivanova I.P., Trofimova S.V., Karpel Vel Leitner N., Aristova N.A., Arkhipova E.V., Burkhina O.E., Sysoeva V.A., Piskaryov I.M. The analysis of active products of spark discharge plasma radiation determining biological effects in tissues. *Sovremennye tehnologii v medicine* 2012; 2: 20–30.

12. Piskarev I.M., Astaf'eva K.A., Ivanova I.P. The effect of pulse UV plasma irradiation of liquid through rat skin. *Biophysics* 2017; 62(4): 547–552, https://doi.org/10.1134/s0006350917040170

13. Spirov G.M., Luk'yanov N.B., Shlepkin S.I., Volkov A.A., Moiseenko A.N., Markevtsev I.M., Ivanova I.P., Zaslavskaya M.I. *Ustroystvo dlya vozdeystviya na bioob"ekt* [Bio-object exposure device]. Patent RU 2358773. 2009.

14. Pikaev A.K. *Dozimetriya v radiatsionnoy khimii* [Dosimetry for radiation chemistry]. Moscow: Nauka; 1975; 147 p.

15. Piskarev I.M., Ivanova I.P., Samodelkin A.G., Ivashchenko M.N. *Initsiirovanie i issledovanie svobodno-radikal'nykh protsessov v biologicheskikh eksperimentakh* [Initiation and investigation of free-radical processes in biological experiments]. Nizhny Novgorod: FGBOU VO Nizhegorodskaya GSKhA; 2016; 140 p.

16. Aitken A., Learmonth M. Estimation of disulfide bonds

using Ellman's reagent. In: *The protein protocols handbook.* Walker J.M. (edsitor). Humana Press; 2002; p. 595–596, https://doi.org/10.1385/1-59259-169-8:595.

17. Piskarev I.M. Reaction in corona discharge plasma between water surface and electrode in air and nitrogen. *Russian Journal of Applied Chemistry* 2001; 75(11): 1997–2001.

18. Piskarev I.M. Production under plasma radiation of a long living complex that decays to peroxynitrite and peroxynitrous acid. *Research Journal of Pharmaceutical, Biological and Chemical Sciences* 2015; 6(6): 1136–1149.